

HIGH-RESOLUTION NANOSIMS STUDIES OF PRESOLAR SILICATES: NEW INSIGHTS INTO THE GALACTIC CHEMICAL EVOLUTION OF MAGNESIUM AND SILICON ISOTOPES. P. Hoppe¹, J. Leitner¹, and J. Kodolányi¹, ¹Max Planck Institute for Chemistry, 55128 Mainz, Germany (peter.hoppe@mpic.de).

Introduction: Primitive Solar System materials contain small quantities of presolar grains that formed in the winds of evolved stars and in the ejecta of stellar explosions [1]. Silicates are the most abundant group of presolar grains with stellar origins [2]. As presolar silicates cannot be chemically separated from meteorites, they can be identified only in situ by ion imaging techniques, preferentially in the NanoSIMS. Presolar silicates have typical sizes of ~150 nm and only a small fraction has sizes >300 nm [3]. Because of potential dilution of isotopic anomalies in presolar silicates by contributions from surrounding material of Solar System origin, useful isotope data could be obtained mostly only for O and to some extent also for Si by employing the high-resolution (≤ 100 nm) Cs^+ primary ion source. In this setup Si suffers from a relatively low secondary ion yield and thus large errors for isotopic ratios. Isotope measurements for other major elements in presolar silicates, e.g., Mg, require measurements with an O^- primary ion source, which, until recently, were limited to 200-300 nm spatial resolution. To circumvent these limitations time-consuming preparation methods (based on FIB) were applied, which, however, led to isotope data with relatively large errors for only a few presolar silicate grains [4, 5].

The new Oregon Physics RF plasma O^- primary ion source, which was recently installed on the Cameca NanoSIMS 50 at MPI for Chemistry, has a much better spatial resolution than the previously used Duoplasmatron and permits carrying out isotope measurements with <100 nm spatial resolution. Here, we report high-resolution Mg and Si isotope measurements with the RF plasma O^- ion source on presolar silicate grains from red giant and/or asymptotic giant branch (AGB) stars previously identified in the Acfer 094, Elephant Moraine (EET) 92161, Meteorite Hills (MET) 00426, and Northwest Africa (NWA) 801 meteorites based on their anomalous O-isotopic compositions [6-8]. Data for ^{25}Mg -rich presolar silicate grains will be presented in a companion abstract by [9].

Experimental: Ten presolar silicate grains, 9 of which belong to O isotope Group 1 and one to Group 2 [10], with sizes from 300 to 450 nm were selected for Mg and Si isotope measurements with the NanoSIMS at MPI for Chemistry. For this purpose a focused O^- ion beam (~0.5 pA, <100 nm) was rastered over $2 \times 2 \mu\text{m}^2$ -sized areas around the presolar silicate grains and positive secondary ion images of ^{24}Mg , ^{25}Mg , ^{26}Mg ,

^{27}Al , and ^{28}Si (session 1; all grains), of ^{24}Mg , ^{27}Al , ^{28}Si , ^{29}Si , and ^{30}Si (session 2; 5 Group 1 grains only), and of ^{24}Mg , ^{27}Al , ^{40}Ca , ^{48}Ti , and ^{56}Fe (session 3, to determine elemental abundances; 5 Group 1 grains and the Group 2 grain) were recorded in multi-collection. Magnesium- and Si-isotopic ratios were normalized to those of the surrounding matrix. For elemental abundances, relative sensitivity factors were taken from a compilation of NanoSIMS data obtained for NBS SRM611 glass.

Results and Discussion: The 9 Group 1 grains from this study have $^{17}\text{O}/^{16}\text{O}$ ratios between 5.7×10^{-4} and 2.4×10^{-3} and $^{18}\text{O}/^{16}\text{O}$ ratios from 1.6×10^{-3} to 2.3×10^{-3} . All grains are relatively low in Al (median $\text{Al}/\text{Mg} = 0.046$; Fig. 1). Given that Group 1 presolar oxides have $^{26}\text{Al}/^{27}\text{Al}$ ratios of <0.01 [1] expected contributions to ^{26}Mg from ^{26}Al decay (half life: 717000 yrs) are only between 0 and 5 %.

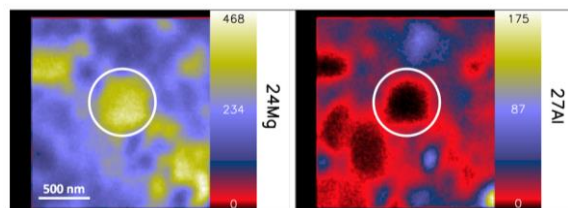


Figure 1. Secondary ion images of $^{24}\text{Mg}^+$ and $^{27}\text{Al}^+$ of presolar silicate grain C@1_21 from Acfer 094 (inside white circle). Based on the elemental distribution maps its chemical composition is close to Fo90. Field of view is $2 \times 2 \mu\text{m}^2$.

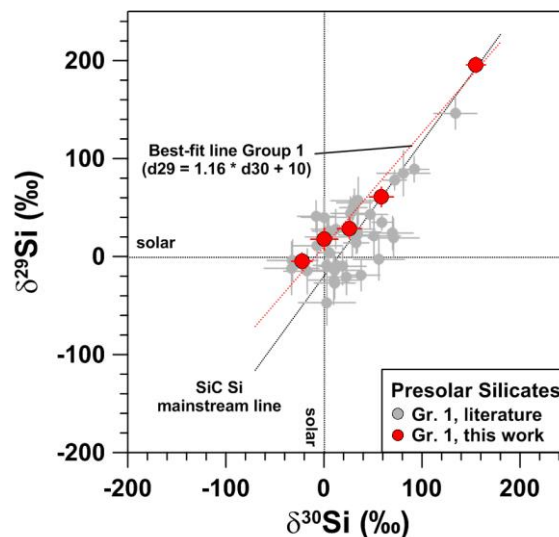


Figure 2. Si-isotopic compositions of Group 1 presolar silicates from this study and selected data (error in $\delta^{30}\text{Si} < 30$ ‰) from previous studies for comparison [2]. Errors are 1σ .

Figure 2 demonstrates that the Si isotope data reported here are much more precise than those obtained previously. The Group 1 grains from this study plot close to the SiC Si mainstream line, although slightly shifted to the ^{30}Si -poor side, in particular for lower $^{29,30}\text{Si}$ enrichments. A best-fit line gives $\delta^{29}\text{Si} = (1.16 \pm 0.06) \times \delta^{30}\text{Si} + (10 \pm 5)$, i.e., it is shallower than the SiC Si mainstream line. Group 1 grains are believed to have formed around 1.2-2.2 M_{\odot} red giant or AGB stars when $\text{C/O} < 1$ [11]. Because silicates form earlier than SiC they are expected to carry less s-process signatures than SiC grains [12]. Their Si can thus be expected to be more representative for the starting composition of Si in their parent stars and a better proxy for the GCE of Si isotopes. However, more presolar silicate data are required to substantiate our finding.

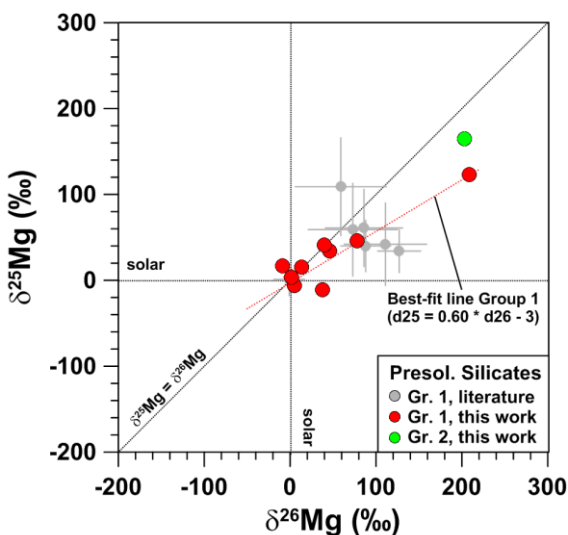


Figure 3. Mg-isotopic compositions of Group 1 and 2 presolar silicates from this study and from [4] for comparison. Errors are 1σ .

As for Si, our Mg isotope data are much more precise than reported previously for presolar silicates (Fig. 3). The 9 Group 1 grains plot along a line $\delta^{25}\text{Mg} = (0.60 \pm 0.02) \times \delta^{26}\text{Mg} + (-3 \pm 2)$. As Mg-isotopic compositions are not expected to change significantly during evolution of low-mass AGB stars [13] and because impacts of ^{26}Al decay, in contrast to presolar spinel grains, are likely only marginal (see above) we consider the observed correlation between $\delta^{25}\text{Mg}$ and $\delta^{26}\text{Mg}$ to represent the GCE of the Mg isotopes and call it the silicate Mg mainstream line. This interpretation is also supported by the good correlation between $\delta^{25}\text{Mg}$ and $\delta^{29}\text{Si}$ (Fig. 4). The observed slope of the silicate Mg mainstream line is lower than the slope ~ 1 predicted by GCE models around solar metallicity [14].

The Group 2 grain ($^{17}\text{O}/^{16}\text{O} = 8.7 \times 10^{-4}$, $^{18}\text{O}/^{16}\text{O} = 7.0 \times 10^{-4}$) plots slightly above the Mg mainstream line (Fig. 3). Group 2 grains are most likely from 4-8 M_{\odot} AGB stars that experienced hot bottom burning (HBB) [15] and the O isotope data of the Group 2 grain reported here are compatible with the predictions for a 6 M_{\odot} AGB star and 35% dilution with matter of solar composition. HBB is expected to lead to large ^{25}Mg and ^{26}Mg enrichments, much larger than observed here, even with consideration of dilution. As discussed by [15] in the context of presolar oxide grains, this may be due to partial equilibration of Mg isotopes in the grains or model deficiencies.

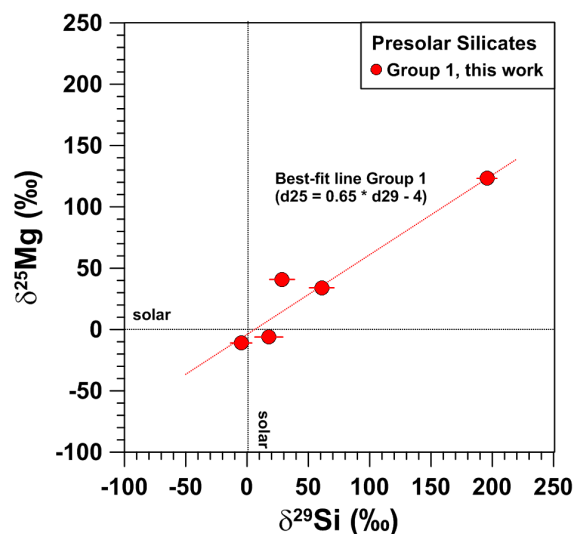


Figure 4. $\delta^{25}\text{Mg}$ vs. $\delta^{29}\text{Si}$ of Group 1 presolar silicates from this study. Errors are 1σ .

Acknowledgements: We thank Antje Sorowka for SEM analyses, Elmar Gröner for technical support on the NanoSIMS, and the NHM Vienna, NHM London, and NASA JSC for the loan of meteorite samples.

References: [1] Zinner E. (2014) Presolar Grains. In *Meteorites and Cosmochemical Processes*, Vol. 1 (ed. A. M. Davis), pp. 181-213. Elsevier. [2] Floss C. and Haenecour P. (2016) *Geochem. J.*, 50, 3-15. [3] Hoppe P. et al. (2017) *Nature Astronomy*, 1, 617-620. [4] Kodolányi J. et al. (2014) *GCA*, 140, 577-605. [5] Nguyen A. et al. (2011) *LPS XLII*, Abstract #2711. [6] Hoppe P. et al. (2015) *ApJ*, 808, L9 (6pp). [7] Leitner J. et al. (2016) *LPS XLVII*, Abstract #1873. [8] Leitner J. et al. (2016) *EPSL*, 434, 117-128. [9] Leitner J. et al. (2018) *LPS XLIX*, this conference. [10] Nittler L. R. et al. (2008) *ApJ*, 682, 1450-1478. [11] Nittler L. R. (2009) *PASA*, 26, 271-277. [12] Zinner E. et al. (2006) *ApJ*, 650, 350-373. [13] Cristallo S. et al. (2015) *ApJS*, 219, 40 (21pp). [14] Kobayashi C. et al. (2011) *MNRAS*, 414, 3231-3250. [15] Lugaro M. et al. (2017) *Nature Astronomy*, 1, 0027.